fractal and fractional

MDPI

Article

The Finite Volume Element Method for Time Fractional Generalized Burgers' Equation

Jingru Zhang and Qing Yang *

School of Mathematics and Statistics, Shandong Normal University, Jinan 250358, China; 17853152910@163.com
* Correspondence: yangqing@sdnu.edu.cn

Abstract: In this paper, we use the finite volume element method (FVEM) to approximate a one-dimensional, time fractional generalized Burgers' equation. We construct the fully discrete finite volume element scheme for this equation by approximating the time fractional derivative term by the $L1$ formula and approximating the spatial terms using FVEM. The convergence of the scheme is proven. Finally, numerical examples are provided to confirm the scheme's validity.

Keywords: finite volume element method; time fractional generalized Burgers' equation; convergence; numerical simulation

check for updates

Citation: Zhang, J.; Yang, Q. The Finite Volume Element Method for Time Fractional Generalized Burgers' Equation. *Fractal Fract.* **2024**, *8*, 53. https://doi.org/10.3390/fractalfract8010053

Academic Editor: Meng Li, Yanmin Zhao, Yang Liu and Haci Mehmet Baskonus

Received: 12 December 2023
Revised: 8 January 2024
Accepted: 12 January 2024
Published: 14 January 2024

Copyright: © 2024 by the authors. Licensee MDPI, Basel, Switzerland. This article is an open access article distributed under the terms and conditions of the Creative Commons Attribution (CC BY) license (https://creativecommons.org/licenses/by/4.0/).

1. Introduction

One of the most well-known nonlinear model equations in the field of fluid dynamics is Burgers' equation. It is obtained from the Navier-Stokes model. These kinds of equations have been studied in the literature using a variety of methods [1–3]. Burgers' equations have been applied in many different areas, including wave propagation, nonlinear acoustics, fluid mechanics and gas dynamics [4–6]. Compared to integer derivatives, fractional-order derivatives often have greater advantages in terms of describing physical processes with memory and genetic properties. Therefore, fractional differential equations are widely used in engineering, environmental science, energy development, physics and many other fields [7–9]. In particular, fractional Burgers' equation is widely used in weak shockwave transmission, compressible turbulence and fluid systems [10–17].

In this article, we consider the time fractional generalized Burgers' equation:

$$(1-q)u_t + q\beta_1 {}_0^C D_t^\alpha u - \gamma \frac{\partial^2 u}{\partial x^2} + \beta_2 u^p \frac{\partial u}{\partial x} = f(x,t), x \in (0,1), t \in (0,T], \tag{1}$$

with the following boundary conditions

$$u(0,t) = u(1,t) = 0, t \in (0,T], \tag{2}$$

and the following initial condition

$$u(x,0) = g(x), x \in (0,1), \tag{3}$$

where $T \in (0,\infty)$, $q \in (0,1)$, β_1, β_2 and γ are constants, and p is a positive integer. The symbol ${}_0^C D_t^\alpha$ of order α is the Caputo fractional derivative operator defined by

$${}_0^C D_t^\alpha u(x,t) = \frac{1}{\Gamma(1-\alpha)} \int_0^t \frac{\partial u(x,s)}{\partial s} \frac{1}{(t-s)^\alpha} ds, 0 < \alpha < 1,$$

where $\Gamma(\cdot)$ denotes the usual Gamma function. In the time fractional generalized Burgers' equation, u is the velocity of the turbulent motion. The first term is the normal change in velocity with respect to time, while the second term is a sub-diffusion term that describes the

change in velocity. The second-order derivative shows the classical diffusion term, which describes how u spreads out over space. The last term on the left-hand side represents nonlinear advection. The right side ($f(x,t) = F(x,t)/\rho$) is a forcing term, where $F(x,t)$ is body force and ρ is density. This equation considers the presence of both normal and sub-diffusion phenomena in the fluid, with q representing the proportion of these two phenomena.

From a physical perspective, the time fractional generalized Burgers' equation can be considered a model of how the chemical substance diffuses across a one-dimensional medium, such a liquid or gas. The SI units of x, u, t, $F(x,t)$ and ρ are m, m/s, s, N/m^3 and kg/m^3, respectively. The diffusion coefficient (γ) controls the rate at which the material spreads out, and its unit is m^2/s. The parameter β_1 represents the sub-diffusion coefficient with SI ($1/s^{1-\alpha}$), and β_2 represents the advection rate with SI ($(m/s)^{1-p}$). They depend on the properties of the material. The temporal memory effect (the substance's past diffusion history impacting its present behavior) in the diffusion process is characterized by the α parameter. In mathematics, dimensionless processing is usually carried out.

In recent years, an increasing number of scholars at home and abroad have carried out numerical research on time fractional Burgers' equations (TFBEs). Li et al. [18,19] proposed the linear implicit finite difference approach for analysis of a generalized TFBE. Esen et al. [20–22] studied this type of problem by means of the finite element method. Zhang and Guo [23] suggested a novel similarity transformation based on the Lie symmetry approach that transforms the TFBE into a fractional ordinary differential equation. Kurt et al. [24] recently discovered the Hopf–Cole transform exact solution to the TFBE, and they obtained an analytical solution using the homotopy analysis method. Cao et al. [25] proposed an approach formed by merging the finite difference method for temporal variables and the discontinuous Galerkin scheme for spatial variables to deal with a two-dimensional TFBE. Liu and Zhang [26] solved this kind of equation using a novel approximation technique named the approximate analytical method.

The finite volume element method (FVEM) is a significant class of numerical methods used to solve differential equations. With a finite partitioning set of volume, this approach discretizes the differential equation using a volume-integral formulation, which is a discrete approximation of the control equation in an integral form. In 2000, Li et al. [27] proposed the use of the FVEM to solve various differential equations. Wang [28] proposed a mixed FVEM to solve biharmonic equations that is based on rectangular partition. Zhang et al. [29] studied a fully discrete two-grid FVEM for a nonlinear parabolic problem. Burgers' equation in one dimension can be solved using a high-order finite volume compact technique, as proposed by Guo et al. [30]. An FVEM for estimation of the solution to a two-dimensional Burgers' equation was proposed by Yang [31]. The FVEM is also widely used in the field of fractional diffusion equations [32–37]. Wang et al. [38] investigated the transverse vibration of a fractional viscoelastic beam using the mixed FVEM. To the best of our knowledge, the FVEM has not been used to investigate the time fractional generalized Burgers' equation, despite the fact that this method has been used for many other Burgers' equations.

Many scholars have investigated the solutions of different kinds of time fractional partial differential equations in the hopes of obtaining effective calculation methods. It is also envisaged that these theoretical analysis and computational approaches may be expanded to sophisticated time fractional models for the solution of additional practical problems. A focus of our studies is the appropriate handling of the nonlinear convection and diffusion factors that are present in various fluid dynamics situations. Here, we provide a theoretical analysis of the time fractional generalized Burgers' equation, which contains time fractional derivatives and nonlinear terms, by using FVEM. Using flexible grids, the FVEM benefits from both the accuracy of the finite element methods and the simplicity of the finite difference methods. In this sense, we have advanced existing knowledge.

The remainder of this article is structured as follows. In Section 2, we construct the fully discrete scheme. In Section 3, some lemmas required for the theoretical analysis are

presented. In Section 4, a convergence analysis of the FVE scheme is provided. Finally, numerical results are presented in Section 5 to confirm our theoretical analysis.

2. Fully Discrete FVE Scheme

Let $T_h : 0 = x_0 < x_1 < x_2 < \cdots < x_N = 1$ be the primal partition of the interval [0, 1] and $I_i = [x_i, x_{i+1}], i = 0, 1, \cdots, N-1$ be the corresponding element intervals. We denote the length of I_i as $h_i = x_{i+1} - x_i$; therefore, $h = \max\limits_{0 \le i \le N-1} h_i$. The corresponding dual partition is $T_h^* : 0 = x_0 < x_{\frac{1}{2}} < x_1 < x_{\frac{3}{2}} \cdots < x_{N-\frac{1}{2}} < x_N = 1$, where $x_{i+\frac{1}{2}} = \dfrac{x_i + x_{i+1}}{2}, i = 0, 1, \cdots, N-1$. The dual elements are $I_0^* = [x_0, x_{\frac{1}{2}}], I_i^* = [x_{i-\frac{1}{2}}, x_{i+\frac{1}{2}}] (i = 1, 2, \cdots, N-1)$ and $I_N^* = [x_{N-\frac{1}{2}}, x_N]$.

The finite element spaces are defined as

$$
\begin{aligned}
&U_h = \left\{u_h \in C(0,1) : u_h|_{I_i} \in P_1, i = 0, 1, \cdots, N-1\right\},\\
&V_h = \left\{v_h \in L^2(0,1) : v_h|_{I_i^*} \in P_0, i = 0, 1, \cdots, N-1\right\},\\
&U_{0h} = \{u_h \in U_h : u_h(0) = u_h(1) = 0\},\\
&V_{0h} = \{v_h \in V_h : v_h(0) = v_h(1) = 0\},
\end{aligned}
$$

where U_h is the linear finite element space according to primal subdivision T_h, and V_h denotes the constant function space corresponding to dual subdivision T_h^*. $P_l (l = 0, 1)$ represents the set of polynomials whose degree is no more than l.

The interpolation operator ($\Pi_h^* : U_{0h} \to V_{0h}$) is expressed as

$$
\Pi_h^* \phi_h = \sum_{i=1}^{N-1} \phi_i \varphi_i(x), \forall \phi_h \in U_{0h},
$$

where $\phi_i = \phi_h(x_i)$ and $\varphi_i(x)$ are the basis functions of V_{0h}, i.e.,

$$
\varphi_i(x) = \begin{cases} 1, x \in I_i^*, \\ \qquad i = 1, 2, \cdots, N-1. \\ 0, x \notin I_i^*. \end{cases}
$$

Any $v_h \in V_{0h}$ has the following form:

$$
v_h = \sum_{i=1}^{N-1} v_i \varphi_i,
$$

where $v_i = v_h(x_i)$. Using any $v_h \in V_{0h}$ to multiply Equation (1) and integrating it on [0, 1], we can obtain

$$
(1-q)(u_t, v_h) + q\beta_1({}_0^C D_t^\alpha u, v_h) + a(u, v_h) + \beta_2(u^p \frac{\partial u}{\partial x}, v_h) = (f, v_h), \tag{4}
$$

where the bilinear form is

$$
a(u, v_h) = -\gamma \sum_{i=1}^{N-1} v_i [u_x(x_{i+\frac{1}{2}}, t) - u_x(x_{i-\frac{1}{2}}, t)].
$$

Using the operator Π_h^*, (4) can also be expressed as

$$
\begin{aligned}
&(1-q)(u_t, \Pi_h^* \phi_h) + q\beta_1({}_0^C D_t^\alpha u, \Pi_h^* \phi_h) + a(u, \Pi_h^* \phi_h) + \beta_2(u^p \frac{\partial u}{\partial x}, \Pi_h^* \phi_h)\\
&= (f, \Pi_h^* \phi_h), \forall \phi_h \in U_h,
\end{aligned} \tag{5}
$$

The semi-discrete FVE scheme of problems (1)–(3) is summarized as follow. For any $t \in [0, T]$, find $u_h(\cdot, t) \in U_{0h}$ such that

$$\begin{cases} (1-q)(u_{ht}, \Pi_h^* \phi_h) + q\beta_1({}_0^C D_t^\alpha u_h, \Pi_h^* \phi_h) + a(u_h, \Pi_h^* \phi_h) + \beta_2(u_h^p \dfrac{\partial u_h}{\partial x}, \Pi_h^* \phi_h) \\ = (f, \Pi_h^* \phi_h), \forall \phi_h \in U_{0h}, \\ u_h(x, 0) = g_h(x), x \in (0, 1), \end{cases} \tag{6}$$

where $g_h(x)$ takes the elliptic projection of $g(x)$.

Then, the subdivision of time interval [0, T] is expressed as $0 = t_0 < t_1 < t_2 < \cdots < t_M = T$, where $t_n = n\tau, \tau = T/M$. The backward difference quotient $(\partial_t u_h(x, t_n) = (u_h(x, t_n)) - u_h(x, t_{n-1}))/\tau)$ is used to approximate u_{ht}. Then, we provide several lemmas related to the Caputo derivative.

Lemma 1 ([39]). *For $0 < \alpha < 1, a_l^{(\alpha)} = (l+1)^{1-\alpha} - l^{1-\alpha}, l = 0, 1, 2, \ldots$, one has*

$$\begin{aligned} &\text{(i) } 1 = a_0^\alpha > a_1^\alpha > a_2^\alpha > \cdots > a_l^\alpha > 0; a_l^\alpha \to 0, l \to \infty; \\ &\text{(ii) } (1-\alpha) l^{-\alpha} < a_{l-1}^\alpha < (1-\alpha)(l-1)^{-\alpha}, l \geq 1. \end{aligned}$$

Lemma 2 ([39]). *For any function $(v(t))$, assume that $v_{tt} \in C(0, T)$. For the Caputo derivative of order $\alpha (0 < \alpha < 1)$, one has*

$$\begin{aligned} {}_0^C D_t^\alpha v^n &= \frac{\tau^{-\alpha}}{\Gamma(2-\alpha)} [a_0^{(\alpha)} v^n - \sum_{k=1}^{n-1} (a_{n-k-1}^{(\alpha)} - a_{n-k}^{(\alpha)}) v^k - a_{n-1}^{(\alpha)} v^0] + R_n \\ &= \frac{\tau^{-\alpha}}{\Gamma(2-\alpha)} \sum_{k=1}^{n} a_{n-k-1}^{(\alpha)} (v^k - v^{k-1}) + R_n, \end{aligned}$$

where $v^n = v(t_n)$, and

$$|R_n| \leq \frac{1}{2\Gamma(1-\alpha)} [\frac{1}{4} + \frac{\alpha}{(1-\alpha)(2-\alpha)}] \max_{t_0 \leq t \leq t_n} |v_{tt}| \tau^{2-\alpha}.$$

We define $r = \dfrac{\tau^{-\alpha}}{\Gamma(2-\alpha)}$, $D_\tau^\alpha v^n = r[a_0^{(\alpha)} v^n - \sum\limits_{k=1}^{n-1} (a_{n-k-1}^{(\alpha)} - a_{n-k}^{(\alpha)}) v^k - a_{n-1}^{(\alpha)} v^0]$. Then, the fully discrete FVE scheme involves fining $u_h^n \in U_{0h} (n = 0, 1, \cdots, M)$, such that

$$\begin{cases} (a)\ (1-q)(\partial_t u_h^n, \Pi_h^* \phi_h) + q\beta_1 (D_\tau^\alpha u_h^n, \Pi_h^* \phi_h) + a(u_h^n, \Pi_h^* \phi_h) + \beta_2((u_h^{n-1})^p \dfrac{\partial u_h^n}{\partial x}, \Pi_h^* \phi_h) \\ = (f^n, \Pi_h^* \phi_h), \forall \phi_h \in U_{0h}, \\ (b)\ u_h^0 = g_h, x \in (0, 1). \end{cases} \tag{7}$$

3. Some Lemmas

In this section, we provide several necessary lemmas. First, we introduce the elliptic projection operator $(P_h : H^2(\Omega) \bigcap H_0^1(\Omega) \to U_{0h})$, which is defined as

$$a(P_h u, v_h) = a(u, v_h), \forall v_h \in V_{0h}.$$

Lemma 3 ([27]). *If $u \in H_0^1(\Omega) \cap H^2(\Omega)$, then*

$$\|u - P_h u\|_1 \leq Ch|u|_2.$$

If $u \in W^{3,p}(\Omega)$, then

$$\|u - P_h u\| \leq Ch^2 |u|_{3,p}, (p > 1).$$

Lemma 4 ([27,40]). *For the operator Π_h^*, we have*

$$\begin{aligned}&\text{(i) } (u_h, \Pi_h^* w_h) = (w_h, \Pi_h^* u_h), \forall u_h, w_h \in U_h,\\ &\text{(ii) } (u_h, \Pi_h^* u_h) \geq 0, \forall u_h \in U_h,\\ &\text{(iii) } |(u_h, \Pi_h^* w_h)| \leq C\|u_h\|\|w_h\|, \forall u_h, w_h \in U_h,\end{aligned}$$

where C is a positive constant. We set $|||u_h||| = (u_h, \Pi_h^* u_h)^{\frac{1}{2}}$; then, $|||\cdot|||$ is equivalent to $\|\cdot\|$ on U_h.

Lemma 5 ([27]). *There exist positive constants (β, C) such that*

$$a(u_h, \Pi_h^* u_h) \geq \beta |u_h|_1^2, \forall u_h \in U_h,$$

$$|a(u_h, \Pi_h^* w_h)| \leq C\|u_h\|_1 \|w_h\|_1, \forall u_h, w_h \in U_h.$$

If we define $|||u_h|||_1 = [a(u_h, \Pi_h^* u_h)]^{\frac{1}{2}}$, then $|||\cdot|||_1$ and $\|\cdot\|_1$ are equivalent on U_h.

Lemma 6 ([27]). *Let $\{z_k\}, \{g_k\}$ be two non-negative sequences. If*

$$z_k \leq K + \sum_{i=1}^{k} g_i z_i, k \geq 0,$$

it holds that

$$z_k \leq K \cdot \exp(\sum_{i=1}^{k} g_i), k \geq 0,$$

where K is a non-negative constant.

4. Convergence Analysis

The error estimate for the fully discrete FVE scheme (7) is discussed in this section.

Theorem 1. *Assume that u and $u_h^n (n = 1, 2, \cdots, N)$ are the solutions to problems (1)–(3) and finite volume element format (7), respectively. If u satisfies the required regularity condition, the following error inequality holds:*

$$\|u^n - u_h^n\| \leq C(\tau + h),$$

where $u^n = u(x, t_n)$, and $C \geq 0$ is a constant independent of the two mesh parameters (τ and h).

Proof. Let

$$\rho^n = u^n - P_h u^n, \eta^n = P_h u^n - u_h^n;$$

then,

$$u^n - u_h^n = \rho^n + \eta^n. \tag{8}$$

According to Lemma 3,

$$\|\rho^n\| = \|u^n - P_h u^n\| \leq Ch^2 \|u^n\|_{3,p} \leq Ch^2 [\|u^0\|_{3,p} + \int_0^{t_n} \|u_t\|_{3,p} dt]. \tag{9}$$

By subtracting (7) from (5), we have the error equation:

$$\begin{aligned}&(1-q)(u_t^n - \partial_t u_h^n, \Pi_h^* \phi_h) + q\beta_1 ({}_0^C D_t^\alpha u^n - D_\tau^\alpha u_h^n, \Pi_h^* \phi_h) + a(u^n - u_h^n, \Pi_h^* \phi_h)\\ &+\beta_2((u_h^n)^p \frac{\partial u_h^n}{\partial x}, \Pi_h^* \phi_h) - \beta_2((u^{n-1})^p \frac{\partial u^n}{\partial x}, \Pi_h^* \phi_h) = 0, \forall \phi_h \in U_{0h}.\end{aligned} \tag{10}$$

Taking $\phi_h = \eta^n$ in the error Equation (10), the error equation becomes

$$
\begin{aligned}
&(1-q)(\partial_t\eta^n,\Pi_h^*\eta^n)+a(\eta^n,\Pi_h^*\eta^n)+q\beta_1 r(\eta^n,\Pi_h^*\eta^n)\\
&=q\beta_1 r\sum_{k=1}^{n-1}(a_{n-k-1}^{(\alpha)}-a_{n-k}^{(\alpha)})(\eta^k,\Pi_h^*\eta^n)+q\beta_1 r a_{n-1}^{(\alpha)}(\eta^0,\Pi_h^*\eta^n)-(1-q)(u_t^n-\partial_t P_h u^n,\Pi_h^*\eta^n)\\
&+q\beta_1(D_\tau^\alpha P_h u^n-{}_0^C D_t^\alpha u^n,\Pi_h^*\eta^n)+\beta_2[((u^n)^p\frac{\partial u^n}{\partial x},\Pi_h^*\eta^n)-((u_h^{n-1})^p\frac{\partial u_h^n}{\partial x},\Pi_h^*\eta^n)].
\end{aligned}
\tag{11}
$$

Noticing the fact that

$$
\begin{aligned}
(\partial_t\eta^n,\Pi_h^*\eta^n)&=\frac{1}{\tau}(\eta^n-\eta^{n-1},\Pi_h^*\eta^n)\\
&=\frac{1}{2\tau}[(\eta^n,\Pi_h^*\eta^n)-(\eta^{n-1},\Pi_h^*\eta^{n-1})+(\eta^n-\eta^{n-1},\Pi_h^*(\eta^n-\eta^{n-1}))]\\
&=\frac{1}{2\tau}(|||\eta^n|||^2-|||\eta^{n-1}|||^2+|||\eta^n-\eta^{n-1}|||^2)\\
&\geq\frac{1}{2\tau}(|||\eta^n|||^2-|||\eta^{n-1}|||^2)
\end{aligned}
$$

and using Lemmas 4 and 5, the left side of Equation (11) is bounded: as follows

$$
\begin{aligned}
&(1-q)(\partial_t\eta^n,\Pi_h^*\eta^n)+a(\eta^n,\Pi_h^*\eta^n)+q\beta_1 r(\eta^n,\Pi_h^*\eta^n)\\
&\geq\frac{1-q}{2\tau}(|||\eta^n|||^2-|||\eta^{n-1}|||^2)+|||\eta^n|||_1^2+q\beta_1 r|||\eta^n|||^2.
\end{aligned}
\tag{12}
$$

The terms on the right side of (11) are denoted as T_1, T_2, T_3, T_4 and T_5, respectively. Using Hölder inequality and Schwarz inequality,

$$
\begin{aligned}
|T_1|&=qr\sum_{k=1}^{n-1}(a_{n-k-1}^{(\alpha)}-a_{n-k}^{(\alpha)})|\beta_1(\eta^k,\Pi_h^*\eta^n)|\\
&\leq Cqr\sum_{k=1}^{n-1}(a_{n-k-1}^{(\alpha)}-a_{n-k}^{(\alpha)})|||\eta^k|||\,|||\eta^n|||\\
&\leq Cqr\sum_{k=1}^{n-1}(a_{n-k-1}^{(\alpha)}-a_{n-k}^{(\alpha)})|||\eta^k|||^2+Cqr(1-a_{n-1}^{(\alpha)})|||\eta^n|||^2.
\end{aligned}
$$

Noticing $P_h u^0=u_h^0$, so $\eta^0=0$, then,

$$
|T_2|=qra_{n-1}^{(\alpha)}|\beta_1(\eta^0,\Pi_h^*\eta^n)|=0.
$$

We denote

$$
\begin{aligned}
\xi^n&=u_t^n-\partial_t u^n+\partial_t u^n-\partial_t P_h u^n\\
&=\xi_1^n+\xi_2^n,
\end{aligned}
$$

where

$$
\begin{aligned}
\|\xi_1^n\|^2&=\int_\Omega(\frac{1}{\tau}\int_{t_{n-1}}^{t_n}(t-t_{n-1})u_{tt}d\tau)^2dx\\
&\leq\tau\int_{t_{n-1}}^{t_n}\|u_{tt}\|^2d\tau,
\end{aligned}
$$

$$\begin{aligned}\|\xi_2^n\|^2 &= \int_\Omega (-\frac{1}{\tau}\int_{t_{n-1}}^{t_n}(P_h - I)u_t d\tau)^2 dx \\ &\le \frac{1}{\tau}\int_{t_{n-1}}^{t_n}\|u_t - P_h u_t\|^2 d\tau \\ &\le \frac{Ch^2}{\tau}\int_{t_{n-1}}^{t_n}|u_t|_2^2 d\tau.\end{aligned}$$

Using Hölder inequality, Schwarz inequality and the above estimates for ξ_1^n and ξ_2^n, we have

$$\begin{aligned}|T_3| &= (1-q)|(u_t^n - \partial_t P_h u^n, \Pi_h^* \eta^n)| \\ &= (1-q)|(\xi^n, \Pi_h^* \eta^n)| \\ &\le C(1-q)|||\xi^n|||^2 + C(1-q)|||\eta^n|||^2 \\ &\le C(1-q)\tau\int_{t_{n-1}}^{t_n}\|u_{tt}\|^2 d\tau + \frac{C(1-q)h^2}{\tau}\int_{t_{n-1}}^{t_n}|u_t|_2^2 d\tau + C(1-q)|||\eta^n|||^2.\end{aligned}$$

We denote

$$\begin{aligned}\epsilon^n &= D_\tau^\alpha P_h u^n - {}_0^C D_t^\alpha u^n \\ &= D_\tau^\alpha P_h u^n - D_\tau^\alpha u^n + D_\tau^\alpha u^n - {}_0^C D_t^\alpha u^n \\ &= \epsilon_1^n + \epsilon_2^n.\end{aligned}$$

According to Lemmas 2 and 3, we have

$$\begin{aligned}\|\epsilon_1^n\|^2 &= (\int_\Omega |\epsilon_1^n|^2 dx) \\ &\le C(n\tau)^{2-2\alpha}\max_{0\le t\le t_n}\|(P_h - I)u_t\|^2 \\ &\le Ch^4(n\tau)^{2-2\alpha}\max_{0\le t\le t_n}\|u_t\|_{3,p}^2,\end{aligned}$$

$$\begin{aligned}\|\epsilon_2^n\| &= (\int_\Omega |\epsilon_2^n|^2 dx) \\ &\le C\tau^{4-2\alpha}\max_{0\le t\le t_n}\|u_{tt}\|^2.\end{aligned}$$

Using the above inequalities, we have

$$\begin{aligned}|T_4| &= q|\beta_1(D_\tau^\alpha P_h u^n - {}_0^C D_t^\alpha u^n, \Pi_h^* \eta^n)| \\ &= q|\beta_1(\epsilon^n, \Pi_h^* \eta^n)| \\ &\le Cq|||\epsilon^n|||^2 + Cq|||\eta^n|||^2 \\ &\le Cqh^4(n\tau)^{2-2\alpha}\max_{0\le t\le t_n}\|u_t\|_{3,p}^2 + Cq\tau^{4-2\alpha}\max_{0\le t\le t_n}\|u_{tt}\|^2 + Cq|||\eta^n|||^2 \\ &\le Cqh^4T^{2-2\alpha}\max_{0\le t\le t_n}\|u_t\|_{3,p}^2 + Cq\tau^{4-2\alpha}\max_{0\le t\le t_n}\|u_{tt}\|^2 + Cq|||\eta^n|||^2.\end{aligned}$$

Then, we estimate $|T_5|$.

$$\begin{aligned}
T_5 =&\beta_2[((u^n)^p\frac{\partial u^n}{\partial x},\Pi_h^*\eta^n)-((u_h^{n-1})^p\frac{\partial u_h^n}{\partial x},\Pi_h^*\eta^n)]\\
=&\beta_2[((u^n)^p\frac{\partial(u^n-P_hu^n)}{\partial x},\Pi_h^*\eta^n)+(((u^n)^p-(u_h^{n-1})^p)\frac{\partial P_hu^n}{\partial x},\Pi_h^*\eta^n)\\
&+((u_h^{n-1})^p\frac{\partial(P_hu^n-u_h^n)}{\partial x},\Pi_h^*\eta^n)]\\
=&\beta_2[((u^n)^p\frac{\partial\rho^n}{\partial x},\Pi_h^*\eta^n)+(((u^n)^p-(u_h^{n-1})^p)\frac{\partial P_hu^n}{\partial x},\Pi_h^*\eta^n)+((u_h^{n-1})^p\frac{\partial\eta^n}{\partial x},\Pi_h^*\eta^n)]\\
=&T_{51}+T_{52}+T_{53}.
\end{aligned}$$

According to Lemma 3,

$$\|\rho^n\|_1\le Ch\|u^n\|_2\le Ch[\|u^0\|_2+\int_0^{t_n}\|u_t\|_2dt].$$

Using Hölder inequality and Schwarz inequality, we can obtain

$$\begin{aligned}
|T_{51}|&=\left|\beta_2((u^n)^p\frac{\partial\rho^n}{\partial x},\Pi_h^*\eta^n)\right|\\
&\le C|||\frac{\partial\rho^n}{\partial x}|||\ |||\eta^n|||\\
&\le C|||\rho^n|||_1^2+C|||\eta^n|||^2\\
&\le Ch^2[\|u^0\|_2+\int_0^{t_n}\|u_t\|_2dt]^2+C|||\eta^n|||^2.
\end{aligned}$$

Therefore, we can make the following inductive hypothesis:

$$\|u_h^{n-1}\|_\infty\le K,1\le n\le N, \tag{13}$$

where $K=\max\limits_{n\tau\le T}\|u^n\|_\infty+1$.

Then, we estimate $|T_{52}|$.

As

$$\begin{aligned}
\|u^n-u_h^{n-1}\|&=\|u^n-u^{n-1}+u^{n-1}-u_h^{n-1}\|\\
&\le\|u^n-u^{n-1}\|+\|\rho^{n-1}\|+\|\eta^{n-1}\|\\
&=(\tau\int_{t_{n-1}}^{t_n}\|u_t\|^2d\tau)^{\frac{1}{2}}+\|\rho^{n-1}\|+\|\eta^{n-1}\|,
\end{aligned}$$

and

$$\begin{aligned}
&\|(u^n)^{p-1}+(u^n)^{p-2}u_h^{n-1}+\cdots+u^n(u_h^{n-1})^{p-2}+(u_h^{n-1})^{p-1}\|\\
&\le C+CK+CK^2+\cdots+CK^{P-2}+K^{P-1}\\
&=C\frac{1-K^p}{1-K},
\end{aligned}$$

we have

$$\begin{aligned}
&\|(u^n)^p-(u_h^{n-1})^p\|\\
=&\|(u^n-u_h^{n-1})((u^n)^{p-1}+(u^n)^{p-2}u_h^{n-1}+\cdots+u^n(u_h^{n-1})^{p-2}+(u_h^{n-1})^{p-1})\|\\
\le&C\frac{1-K^p}{1-K}[(\tau\int_{t_{n-1}}^{t_n}\|u_t\|^2dt)^{\frac{1}{2}}+\|\rho^{n-1}\|+\|\eta^{n-1}\|].
\end{aligned}$$

Using Lemma 4, Hölder inequality and Schwarz inequality, we can obtain

$$\begin{aligned}|T_{52}| &= |\beta_2((u^n)^p - (u_h^{n-1})^p \frac{\partial P_h u^n}{\partial x}, \Pi_h^* \eta^n)| \\ &\le C\|(u^n)^p - (u_h^{n-1})^p\| \, |||\eta^n||| \\ &\le C\frac{1-K^p}{1-K}[(\tau \int_{t_{n-1}}^{t_n} \|u_t\|^2 dt)^{\frac{1}{2}} + \|\rho^{n-1}\| + \|\eta^{n-1}\|]|||\eta^n||| \\ &\le C\frac{1-K^p}{1-K}\tau \int_{t_{n-1}}^{t_n} \|u_t\|^2 dt + C\frac{1-K^p}{1-K}h^2[\|u^0\|_{3,p} + \int_0^{t_n} \|u_t\|_{3,p} dt]^2 \\ &+ C\frac{1-K^p}{1-K}\|\eta^{n-1}\|^2 + C\frac{1-K^p}{1-K}|||\eta^n|||^2.\end{aligned}$$

According to our induction hypothesis, Hölder inequality and ε-inequality, we have

$$\begin{aligned}|T_{53}| &= \left|\beta_2((u_h^{n-1})^p \frac{\partial \eta^n}{\partial x}, \Pi_h^* \eta^n)\right| \\ &\le C|||\eta^n|||_1|||\eta^n||| \\ &\le \varepsilon|||\eta^n|||_1^2 + \frac{C}{4\varepsilon}|||\eta^n|||^2.\end{aligned}$$

Substituting the above estimates of T_{51}, T_{52} and T_{53} into T_5, we have

$$\begin{aligned}|T_5| \le\ & Ch^2[\|u^0\|_2 + \int_0^{t_n} \|u_t\|_2 dt]^2 + C\frac{1-K^p}{1-K}\tau \int_0^T \|u_t\|^2 dt \\ &+ C\frac{1-K^p}{1-K}h^2[\|u^0\|_{3,p} + \int_0^{t_n} \|u_t\|_{3,p} dt]^2 + C\frac{1-K^p}{1-K}\|\eta^{n-1}\|^2 + C\frac{1-K^p}{1-K}|||\eta^n|||^2 \\ &+ C|||\eta^n|||^2 + \varepsilon|||\eta^n|||_1^2 + \frac{C}{4\varepsilon}|||\eta^n|||^2.\end{aligned}$$

Combining estimates of T_1, T_2, T_3, T_4, T_5 and (12), we can obtain

$$\begin{aligned}&\frac{1-q}{2\tau}(|||\eta^n|||^2 - |||\eta^{n-1}|||^2) + |||\eta^n|||_1^2 + \beta_1 qr|||\eta^n|||^2 \\ &\le Cqr\sum_{k=1}^{n-1}(a_{n-k-1}^{(\alpha)} - a_{n-k}^{(\alpha)})|||\eta^k|||^2 + Cqr(1 - a_{n-1}^{(\alpha)})|||\eta^n|||^2 \\ &+C(1-q)\tau \int_{t_{n-1}}^{t_n} \|u_{tt}\|^2 dt + \frac{C(1-q)h^2}{\tau} \int_{t_{n-1}}^{t_n} |u_t|_2^2 dt + Cqh^4 T^{2-2\alpha} \max_{0\le t\le t_n} \|u_t\|_{3,p}^2 \\ &+Cq\tau^{4-2\alpha} \max_{0\le t\le t_n} \|u_{tt}\|^2 + Ch^2[\|u^0\|_2 + \int_0^{t_n} \|u_t\|_2 dt]^2 + C\frac{1-K^p}{1-K}\tau \int_{t_{n-1}}^{t_n} \|u_t\|^2 dt \\ &+C\frac{1-K^p}{1-K}h^2[\|u^0\|_{3,p} + \int_0^{t_n} \|u_t\|_{3,p} dt]^2 + C\frac{1-K^p}{1-K}\|\eta^{n-1}\|^2 + C\frac{1-K^p}{1-K}|||\eta^n|||^2 \\ &+C|||\eta^n|||^2 + \varepsilon|||\eta^n|||_1^2 + \frac{C}{4\varepsilon}|||\eta^n|||^2.\end{aligned} \tag{14}$$

Let $\varepsilon = 1$, $\tilde{C} = C\frac{1-K^p}{1-K}$, and multiply both sides of inequality (14) by $\frac{2\tau}{1-q}$; then, (14) is equivalent to

$$
\begin{aligned}
&|||\eta^n|||^2 \le \frac{Cq\tau^{1-\alpha}}{1-q}\sum_{k=1}^{n-1}(a_{n-k-1}^{(\alpha)}-a_{n-k}^{(\alpha)})|||\eta^k|||^2+(1+\tilde{C}\frac{\tau}{1-q})|||\eta^{n-1}|||^2\\
&+\frac{Cq\tau}{1-q}|||\eta^n|||^2+\tilde{C}\frac{\tau}{1-q}|||\eta^n|||^2+\frac{C\tau}{1-q}|||\eta^n|||^2\\
&+\frac{Cq\tau^{1-\alpha}}{(1-q)\Gamma(2-\alpha)}(1-a_{n-1}^{(\alpha)})|||\eta^n|||^2+C\tau^2\int_0^T\|u_{tt}\|^2dt+Ch^2\int_0^T|u_t|_2^2dt\\
&+\frac{Cqh^4T^{3-2\alpha}}{1-q}\max_{0\le t\le t_n}\|u_t\|_{3,p}^2+\frac{Cq\tau^{5-2\alpha}}{1-q}\max_{0\le t\le t_n}\|u_{tt}\|^2+\frac{C\tau h^2}{1-q}[\|u^0\|_2+\int_0^T\|u_t\|_2dt]^2\\
&+\tilde{C}\frac{\tau^2}{1-q}\int_{t^{n-1}}^{t^n}\|u_t\|dt+\tilde{C}\frac{\tau h^2}{1-q}[\|u^0\|_{3,p}+\int_0^T\|u_t\|_{3,p}dt]^2.
\end{aligned}
\tag{15}
$$

Using Lemma 1, we know that

$$\sum_{k=1}^{n-1}(a_{n-k-1}^{(\alpha)}-a_{n-k}^{(\alpha)})=1-a_{n-1}^{(\alpha)}\ge 0.$$

Applying Lemma 6, we have

$$\|\eta^n\|^2\le C_1(\tau^2+h^2)\cdot \exp C_2, \tag{16}$$

where

$$
\begin{aligned}
C_1=&\max\{C\int_0^T\|u_{tt}\|^2dt, C\int_0^T|u_t|_2^2dt, \frac{Cqh^2T^{3-2\alpha}}{1-q}\max_{0\le t\le t_n}\|u_t\|_{3,p}^2,\\
&\frac{CqT^{3-2\alpha}}{1-q}\max_{0\le t\le t_n}\|u_{tt}\|^2, \frac{CT}{1-q}[\|u^0\|_2+\int_0^T\|u_t\|_2dt]^2, \frac{\tilde{C}}{1-q}\int_0^T\|u_t\|d\tau,\\
&\frac{\tilde{C}T}{1-q}\int_0^T\|u_t\|_{3,p}^2dt\},
\end{aligned}
$$

$$
\begin{aligned}
C_2=&1+\frac{Cq\tau^{1-\alpha}}{1-q}(1-a_{n-1}^{(\alpha)})+\frac{Cq\tau^{1-\alpha}}{(1-q)\Gamma(2-\alpha)}(1-a_{n-1}^{(\alpha)})+\frac{Cq\tau}{1-q}\\
&+\frac{C\tau}{1-q}+2\tilde{C}\frac{\tau}{1-q}.
\end{aligned}
$$

Then, we prove the induction hypothesis (13) is true. When $i=0$, this is obviously true. Suppose that the conclusion holds if $i=n-1$. Therefore, when $i=n$, according to the estimate (16), we have $\|\eta^n\|\le\hat{C}(\tau+h)$. Restricting $\tau=O(h)$ and using the inverse estimate, we obtain

$$
\begin{aligned}
\|u_h^n\|_\infty&\le\|P_hu^n\|_\infty+\|\eta^n\|_\infty\\
&\le\|u^n\|_\infty+\hat{C}h^{-\frac{1}{2}}\|\eta^n\|\\
&\le\|u^n\|_\infty+\hat{C}h^{-\frac{1}{2}}(h+\tau)\\
&\le\|u^n\|_\infty+1\\
&\le K,
\end{aligned}
$$

for sufficiently small h, where $\hat{C}=\frac{1}{2}C_1^{\frac{1}{2}}\cdot\exp C_2$. Therefore, induction hypothesis (13) is valid for any n. Finally, according to the triangle inequality, we can obtain

$$\|u^n-u_h^n\|\le\|\rho^n\|+\|\eta^n\|\le Ch^2[\|u^0\|_{3,p}+\int_0^{t_n}\|u_t\|_{3,p}dt]+\hat{C}(\tau+h).$$

The theorem is proven. □

5. Numerical Examples

In this section, we present two numerical examples to gain insights into the theoretical results established in previous sections. The effectiveness and accuracy order of the FVE scheme are shown by numerical results.

Example 1. *Let the parameters* $q = \gamma = \frac{1}{2}$, $\beta_1 = \beta_2 = 1$ *and* $p = 3$ *in problem (1) be defined as:*

$$\frac{1}{2}u_t + \frac{1}{2}\,{}_0^C D_t^{\alpha} u - \frac{1}{2}\frac{\partial^2 u}{\partial x^2} + u^3\frac{\partial u}{\partial x} = f(x,t), x \in (0,1), t \in (0,1],$$

with the following boundary conditions:

$$u(0,t) = u(1,t) = 0, t \in (0,1],$$

and the following initial condition:

$$u(x,0) = g(x), x \in (0,1).$$

We set $f(x,t) = (\frac{\Gamma(5)}{2\Gamma(5-\alpha)}t^{4-\alpha} + 2t^3 + \frac{1}{2}\pi^2 t^4)sin(\pi x) + \pi t^{16} sin^3(\pi x)cos(\pi x)$*; then, we can deduce the exact solution for* $u(x,t) = t^4 sin(\pi x)$*. The spatial step is fixed by* $h = 0.001$*. The time-step length is set as* $\tau = 1/10, 1/20, 1/40, 1/80$*. We present the error and temporal convergence order in Table 1. The* L^2*-norm error between the exact solution (u) and the numerical solution* (u_h) *is defined as* $e(h,\tau) = \sqrt{h\sum_{i=1}^{m-1}[u_i^n - u_h(x_i,t_n)]^2}$*. The result is consistent with the theoretical result reported in Theorem 1, which shows that the convergence order in time is approximately one.*

Table 1. L^2-norm errors and temporal convergence order of the FVEM.

τ	$\alpha = 0.7$ $\|u - u_h\|$	Order	$\alpha = 0.3$ $\|u - u_h\|$	Order
1/10	0.0374	-	0.0311	-
1/20	0.0185	1.0155	0.0158	0.9770
1/40	0.0090	1.0395	0.0079	1.0000
1/80	0.0044	1.0324	0.0040	0.9819

Next, we set the time step as $\tau = \frac{1}{M}$ *and the spatial step as* $h = \frac{1}{N}$*. In order to show the capability of our method, when* $M = N^2$*, we present the spatial convergence orders and errors obtained by the FVEM in Table 2 and those obtained by the finite difference method in Table 3. Table 2 shows that the spatial convergence orders are higher than the theoretical analysis, while Table 3 shows that the finite difference method is less accurate than the FVEM, which proves the effectiveness of the FVEM.*

Table 2. L^2-norm errors and spatial convergence order of the FVEM.

h	$\alpha = 0.7$ $\|u - u_h\|$	Order	$\alpha = 0.3$ $\|u - u_h\|$	Order
1/8	0.0121	-	0.0113	-
1/16	0.0029	2.0609	0.0028	2.0128
1/32	7.2541×10^{-4}	1.9992	7.0135×10^{-4}	1.9972
1/64	4.2090×10^{-4}	2.0162	1.7525×10^{-4}	2.0007

Table 3. L^2-norm errors and spatial convergence order of the finite-difference method.

h	$\alpha = 0.7$ $\|u - u_h\|$	Order	$\alpha = 0.3$ $\|u - u_h\|$	Order
1/8	0.0299	-	0.0300	-
1/16	0.0109	1.4558	0.0107	1.0310
1/32	0.0039	1.4828	0.0038	1.0352
1/64	0.0014	1.4780	0.0013	1.0726

Functional images of the exact solution (u) and the numerical solution (u_h) for $\alpha = 0.7$ are presented in Figure 1, and surface plots are provided in Figures 2–4. As can be seen, there is good agreement between the exact solution and the numerical solution. Figure 5 describes the behavior of absolute errors at t = 1 for h = 1/8, 1/16 and 1/32 and for $\alpha = 0.3$. This shows that error decreases as the number of nodes is increased. Figure 6 shows a comparison of approximated and exact values for h = 0.02, $\tau = 1/80$ and $\alpha = 0.3$ at time levels t = 0.25, 0.5, 0.75 and t = 1.

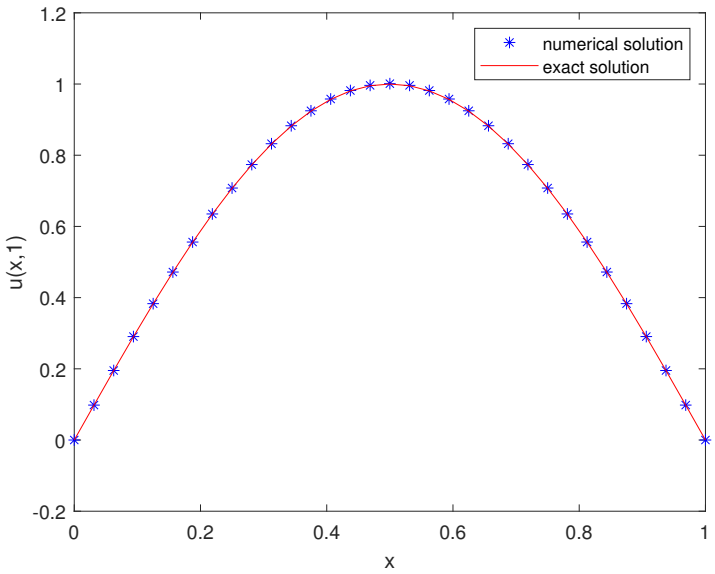


Figure 1. The numerical solution (u_h) and the exact solution (u) at t = 1 for $\alpha = 0.7$ and h = 1/32.

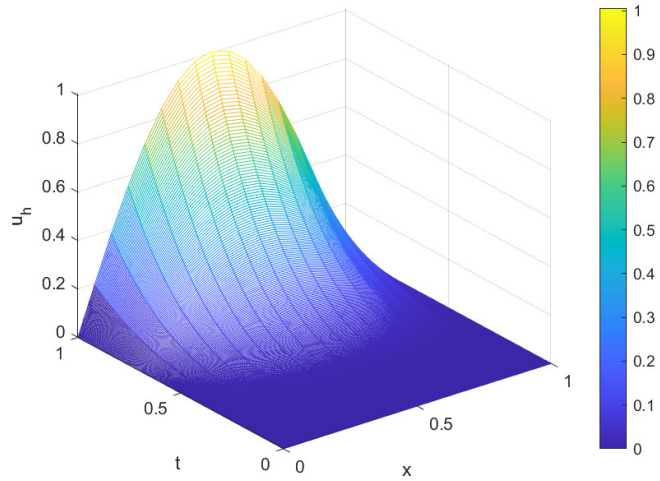


Figure 2. The numerical solution (u_h) for $\alpha = 0.7$ and h = 1/16.

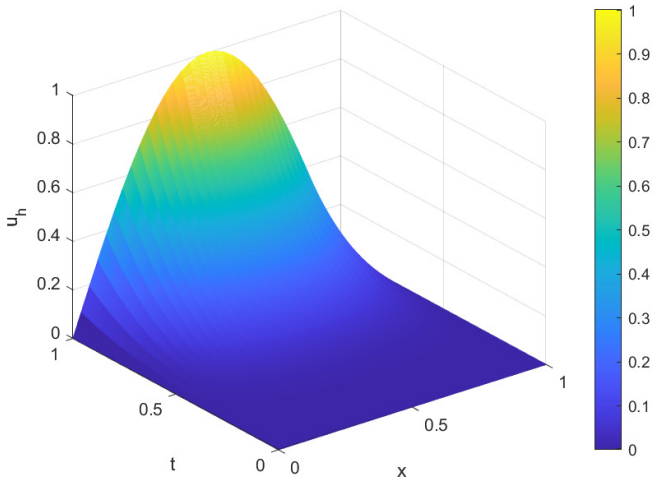


Figure 3. The numerical solution (u_h) for $\alpha = 0.7$ and h = 1/32.

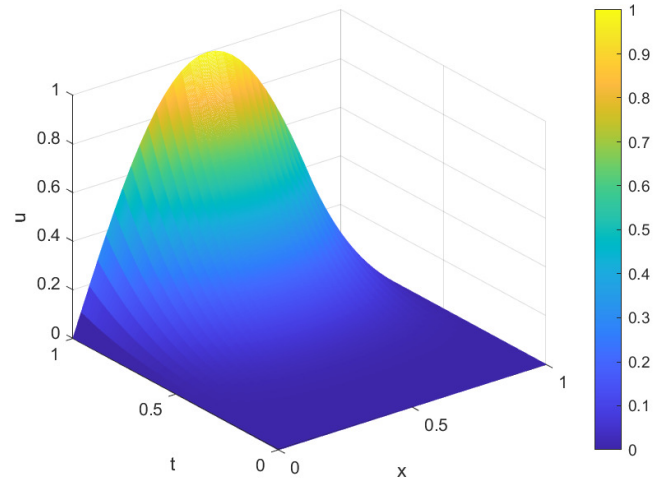


Figure 4. The exact solution (u).

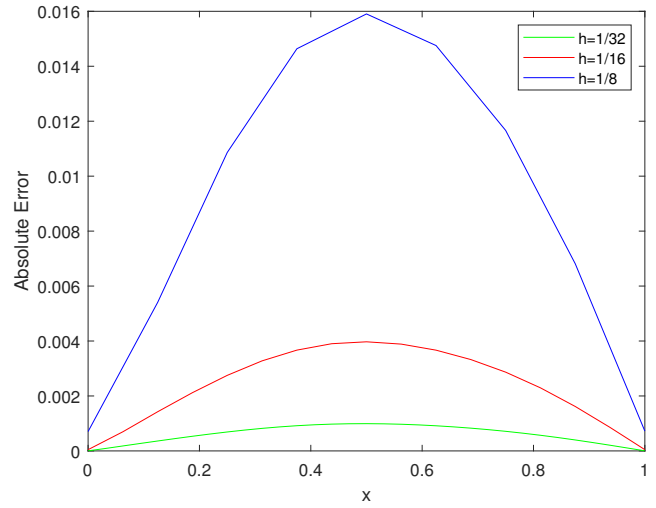


Figure 5. Graph of errors for different h values.

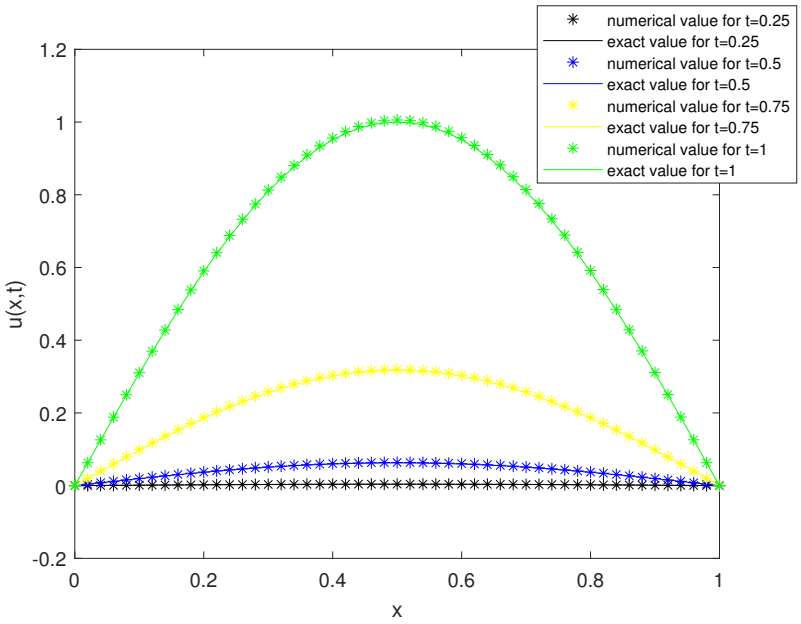


Figure 6. A comparison of the exact and numerical values for various time levels.

Example 2. *In this example, a generalized time fractional Burgers' equation with an unknown exact solution is considered:*

$$\frac{1}{2}u_t + \frac{1}{2}\,{}_0^C D_t^{\alpha} u - \frac{1}{2}\frac{\partial^2 u}{\partial x^2} + u^2\frac{\partial u}{\partial x} = 0, x \in (0,1), t \in (0,T],$$

with following boundary conditions:

$$u(0,t) = u(1,t) = 0, t \in (0,T],$$

and the following initial condition:

$$u(x,0) = sin(\pi x), x \in (0,1),$$

where $T = 1$. In this example, the exact solution is not known beforehand, so we take the numerical solution with $h = 1/150$ as the reference solution to calculate the error and convergence rate. The experimental rates of convergence associated with the mesh size (h) can be calculated using the formula $log(e_i/e_{i+1})/log(h_i/h_{i+1})$, where e_i and e_{i+1} are the relative errors corresponding to mesh of sizes h_i and h_{i+1}, respectively. In Table 4, we present the numerical results for $\alpha = 0.2$ and 0.8. As shown in the table, the format is convergent with one order of accuracy. Surface plots of the reference solution (u) and the numerical solution (u_h) for $\alpha = 0.8$ are presented in Figures 7 and 8, respectively. As evidenced by the table and figures, these results are consistent with the results of our theoretical analysis.

Table 4. Numerical results for $\alpha = 0.2$ and $\alpha = 0.8$.

	$\alpha = 0.2$		$\alpha = 0.8$	
h	$\|u - u_h\|$	**Order**	$\|u - u_h\|$	**Order**
1/25	1.4567×10^{-4}	-	5.8463×10^{-4}	-
1/30	1.2661×10^{-4}	0.7693	5.0481×10^{-4}	0.8220
1/50	8.0646×10^{-5}	0.8829	3.1350×10^{-4}	0.9325
1/75	4.9139×10^{-5}	1.2218	1.8788×10^{-4}	1.2626

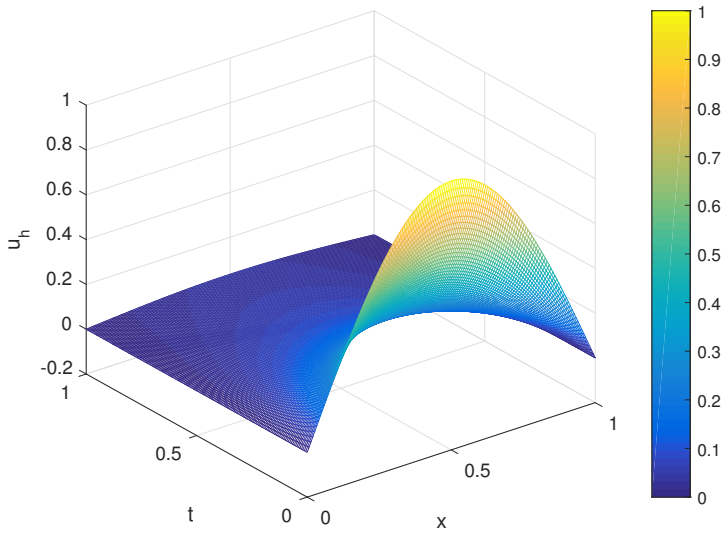


Figure 7. The reference solution (u_h) for $\alpha = 0.8$ and h = 1/150.

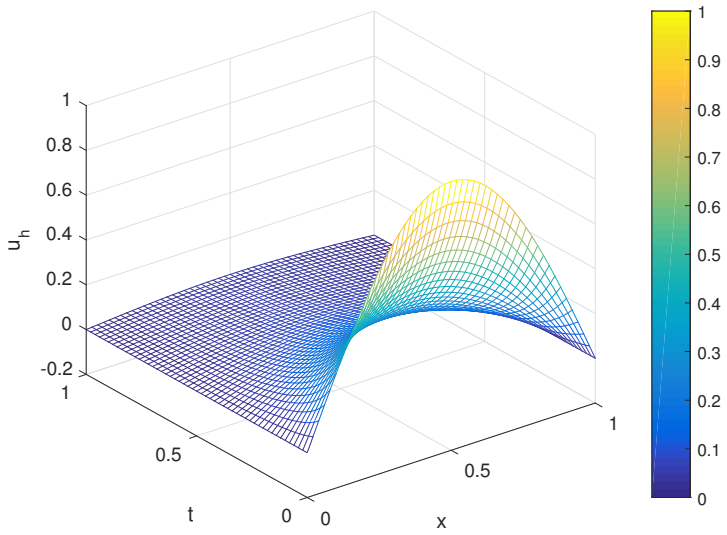


Figure 8. The numerical solution (u_h) for $\alpha = 0.8$ and h = 1/30.

6. Conclusions

In this paper, a fully discrete finite volume element scheme for time fractional generalized Burgers' equations is presented. The convergence of the numerical method is proven herein. In order to verify our theoretical results, two numerical results are presented.

While several approaches exist to address these kinds of issues, the FVEM demonstrates the following benefits: (i) Its accuracy is higher than that of finite difference methods and almost equal to that of finite element methods, while the computational cost is less than that of finite element methods. (ii) The mass conservation law is upheld, which is generally preferable for calculations involving fluids and subterranean fluids, among other things. (iii) The space smoothness requirement is less compared to that of the finite-element method.

However, prior research suggests that it is possible to loosen the smoothness condition of the fractional-order issue solution. To enhance the application of the FVEM, in the future, we will investigate a case of non-smooth data. Furthermore, to increase the method's accuracy, the time derivatives can also be discretized using different techniques.

Author Contributions: Conceptualization, Q.Y.; Writing—original draft, J.Z.; Writing—review and editing, J.Z. and Q.Y. All authors have read and agreed to the published version of the manuscript.

Funding: This work was supported by the National Science Foundation of China (12172202).

Institutional Review Board Statement: Not applicable.

Informed Consent Statement: Not applicable.

Data Availability Statement: Data are contained within the article.

Conflicts of Interest: The authors declare no conflicts of interest

References

1. Öziş, T.; Aksan, E.N.; Özdeş, A. A finite element approach for solution of Burgers' equation. *Appl. Math. Comput.* **2003**, *139*, 417–428. [CrossRef]
2. Dhawan, S.; Kapoor, S.; Kumar, S.; Rawat, S. Contemporary review of techniques for the solution of nonlinear Burgers equation. *J. Comput. Sci.* **2012**, *3*, 405–419. [CrossRef]
3. Khater, A.H.; Temsah, R.S.; Hassan, M.M. A Chebyshev spectral collocation method for solving Burgers'-type equations. *J. Comput. Appl. Math.* **2008**, *222*, 333–350. [CrossRef]
4. Oz, F.; Vuppala, R.K.; Kara, K.; Gaitan, F. Solving Burgers' equation with quantum computing. *Quantum Inf. Process.* **2022**, *21*, 30. [CrossRef]
5. Fu, F.; Li, J.; Lin, J.; Guan, Y.; Gao, F.; Zhang, C.; Chen, L. Moving least squares particle hydrodynamics method for Burgers' equation. *Appl. Math. Comput.* **2019**, *356*, 362–378. [CrossRef]
6. Seadawy, A.R.; Iqbal, M.; Lu, D. Propagation of long-wave with dissipation and dispersion in nonlinear media via generalized Kadomtsive–Petviashvili modified equal width-Burgers equation. *Indian J. Phys.* **2020**, *94*, 675–687. [CrossRef]
7. Jafari, H.; Babaei, A.; Banihashemi, S. A novel approach for solving an inverse reaction-diffusion-convection problem. *J. Optim. Theory Appl.* **2019**, *183*, 688–704. [CrossRef]
8. Nikan, O.; Jafari, H.; Golbabai, A. Numerical analysis of the fractional evolution model for heat flow in materials with memory. *Alex. Eng. J.* **2020**, *59*, 2627–2637. [CrossRef]
9. Mitkowski, W. Approximation of fractional diffusion-wave equation. *Acta Mech. Autom.* **2011**, *5*, 65–68.
10. Momani, S. Non-perturbative analytical solutions of the space-and time-fractional Burgers equations. *Chaos Solitons Fractals* **2006**, *28*, 930–937. [CrossRef]
11. Uddin, M.H.; Arefin, M.A.; Akbar, M.A.; Inc, M. New explicit solutions to the fractional-order Burgers' equation. *Math. Probl. Eng.* **2021**, *2021*, 6698028. [CrossRef]
12. Esen, A.; Bulut, F.; Oruç, Ö. A unified approach for the numerical solution of time fractional Burgers' type equations. *Eur. Phys. J. Plus* **2016**, *131*, 116. [CrossRef]
13. Wang, X.; Wang, L. Traveling wave solutions of conformable time fractional Burgers type equations. *Aims Math* **2021**, *6*, 7266–7284. [CrossRef]
14. Abdelwahed, H.G.; El-Shewy, E.K.; Mahmoud, A.A. On the time fractional modulation for electron acoustic shock waves. *Chin. Phys. Lett.* **2017**, *34*, 035202. [CrossRef]
15. Garra, R. Fractional-calculus model for temperature and pressure waves in fluid-saturated porous rocks. *Phys. Rev. E* **2011**, *84*, 036605. [CrossRef]
16. Keller, J.J. Propagation of simple nonlinear waves in gas filled tubes with friction. *Z. FüR Angew. Math. Phys. ZAMP* **1981**, *32*, 170–181. [CrossRef]
17. Sugimoto, N. Burgers equation with a fractional derivative; Hereditary effects on non-linear acoustic waves. *J. Fluid Mech.* **1991**, *225*, 631–653. [CrossRef]
18. Li, D.; Zhang, C.; Ran, M. A linear finite difference scheme for generalized time fractional Burgers equation. *Appl. Math. Model.* **2016**, *40*, 6069–6081. [CrossRef]
19. Qiu, W.; Chen, H.; Zheng, X. An implicit difference scheme and algorithm implementation for the one-dimensional time-fractional Burgers equations. *Math. Comput. Simul.* **2019**, *166*, 298–314. [CrossRef]
20. Esen, A.; Tasbozan, O. Numerical solution of time fractional Burgers equation by cubic B-spline finite elements. *Mediterr. J. Math.* **2016**, *13*, 1325–1337. [CrossRef]
21. Hussein, A.J. A weak Galerkin finite element method for solving time-fractional coupled Burgers' equations in two dimensions. *Appl. Numer. Math.* **2020**, *156*, 265–275. [CrossRef]
22. Wang, H.; Xu, D.; Zhou, J.; Guo, J. Weak Galerkin finite element method for a class of time fractional generalized Burgers' equation. *Numer. Methods Partial. Differ. Equ.* **2021**, *37*, 732–749. [CrossRef]
23. Zhang, Z.Y.; Guo, L.L. An alternative technique for the symmetry reduction of time-fractional partial differential equation. *Math. Methods Appl. Sci.* **2021**, *44*, 14957–14962. [CrossRef]
24. Kurt, A.; Çenesiz, Y.; Tasbozan, O. On the solution of Burgers' equation with the new fractional derivative. *Open Phys.* **2015**, *13*, 355–360. [CrossRef]

25. Cao, W.; Xu, Q.; Zheng, Z. Solution of two-dimensional time-fractional Burgers equation with high and low Reynolds numbers. *Adv. Differ. Equ.* **2017**, *2017*, 338. [CrossRef]
26. Liu, J.G.; Zhang, J. A new approximate method to the time fractional damped Burger equation. *AIMS Math.* **2023**, *8*, 13317–13324. [CrossRef]
27. Li, R.; Chen, Z.; Wu, W. *Generalized Difference Methods for Differential Equations: Numerical Analysis of Finite Volume Methods*; CRC Press: Boca Raton, FL, USA, 2000.
28. Wang, T. A mixed finite volume element method based on rectangular mesh for biharmonic equations. *J. Comput. Appl. Math.* **2004**, *172*, 117–130. [CrossRef]
29. Zhang, T.; Zhong, H.; Zhao, J. A full discrete two-grid finite-volume method for a nonlinear parabolic problem. *Int. J. Comput. Math.* **2011**, *88*, 1644–1663. [CrossRef]
30. Guo, Y.; Shi, Y.; Li, Y. A fifth-order finite volume weighted compact scheme for solving one-dimensional Burgers' equation. *Appl. Math. Comput.* **2016**, *281*, 172–185. [CrossRef]
31. Yang, Q. The upwind finite volume element method for two-dimensional Burgers equation. In *Abstract and Applied Analysis*; Hindawi Press: London, UK, 2013.
32. Liu, F.; Zhuang, P.; Turner, I.; Burrage, K.; Anh, V. A new fractional finite volume method for solving the fractional diffusion equation. *Appl. Math. Model.* **2014**, *38*, 3871–3878. [CrossRef]
33. Hejazi, H.; Moroney, T.; Liu, F. Stability and convergence of a finite volume method for the space fractional advection—Dispersion equation. *J. Comput. Appl. Math.* **2014**, *255*, 684–697. [CrossRef]
34. Sayev, K.; Arjang, F. Finite volume element method and its stability analysis for analyzing the behavior of sub-diffusion problems. *Appl. Math. Comput.* **2016**, *290*, 224–239.
35. Li, J.; Liu, F.; Feng, L.; Turner, I. A novel finite volume method for the Riesz space distributed-order advection—Diffusion equation. *Appl. Math. Model.* **2017**, *46*, 536–553. [CrossRef]
36. Fu, H.; Sun, Y.; Wang, H.; Zheng, X. Stability and convergence of a Crank–Nicolson finite volume method for space fractional diffusion equations. *Appl. Numer. Math.* **2019**, *139*, 38–51. [CrossRef]
37. Fu, H.; Liu, H.; Wang, H. A finite volume method for two-dimensional Riemann-Liouville space-fractional diffusion equation and its efficient implementation. *J. Comput. Phys.* **2019**, *388*, 316–334. [CrossRef]
38. Wang, T.; Jiang, Z.; Zhu, A.; Yin, Z. A Mixed Finite Volume Element Method for Time-Fractional Damping Beam Vibration Problem. *Fractal Fract.* **2022**, *6*, 523. [CrossRef]
39. Sun, Z.; Wu, X. A fully discrete difference scheme for a diffusion-wave system. *Appl. Numer. Math.* **2006**, *56*, 193–209. [CrossRef]
40. Zhang, T.; Guo, Q. The finite difference/finite volume method for solving the fractional diffusion equation. *J. Comput. Phys.* **2018**, *375*, 120–134. [CrossRef]

Disclaimer/Publisher's Note: The statements, opinions and data contained in all publications are solely those of the individual author(s) and contributor(s) and not of MDPI and/or the editor(s). MDPI and/or the editor(s) disclaim responsibility for any injury to people or property resulting from any ideas, methods, instructions or products referred to in the content.